Biological Invasions (2005) 7: 771–793
DOI 10.1007/s10530-005-5217-7

Patterns of patchy spread in deterministic and stochastic models of biological invasion and biological control

Sergei V. Petrovskii[1,*], Horst Malchow[2], Frank M. Hilker[2] & Ezio Venturino[3]
[1]*Shirshov Institute of Oceanology, Russian Academy of Science, Nakhimovsky Prosp. 36, Moscow 117218, Russia;* [2]*Department of Mathematics and Computer Science, Institute for Environmental Systems Research, University of Osnabrück, 49069 Osnabrück, Germany;* [3]*Department of Mathematics, University of Torino, Via Carlo Alberto 10, Torino 10123, Italy; *Author for correspondence (e-mail: spetrovs@sio.rssi.ru; fax: +7-095-124-5983)*

Received 19 October 2004; accepted in revised form 22 February 2005

Key words: biological control, biological invasion, extinction, infection, patchy invasion, predation

Abstract

A few spatiotemporal models of population dynamics are considered in relation to biological invasion and biological control. The patterns of spread in one and two spatial dimensions are studied by means of extensive numerical simulations. We show that, in the case that population multiplication is damped by the strong Allee effect (when the population growth rate becomes negative for small population density), in a certain parameter range the spread can take place not via the intuitively expected circular expanding population front but via motion and interaction of separate patches. Alternatively, the patchy spread can take place in a system without Allee effect as a result of strong environmental noise. We then show that the phenomenon of deterministic patchy invasion takes place 'at the edge of extinction' so that a small change of controlling parameters either brings the species to extinction or restores the travelling population fronts. Moreover, we show that the regime of patchy invasion in two spatial dimensions actually takes place when the species go extinct in the corresponding 1-D system.

Introduction

Biological invasions are currently regarded as a major threat to biodiversity (Drake et al. 1989; Parker et al. 1999), agriculture (Pimentel 2002), fish stocks (Vinogradov et al. 1989, 2000), etc. The apparent importance of this issue has given rise to various strategies for the management and control of invasive species. The effectiveness of controlling efforts strongly depends on our knowledge of the main feedbacks in a given ecosystem. In particular, the concept of biological control is based on the assumption that the impact of certain biological factors can slow down or block the spread of exotic species. Several factors have been identified that affect the rate and pattern of species spread, including environmental heterogeneity, global climatic change and large-scale phenomena such as El Niño, impact of wind or water current, transport and trade, and others.

From the point of applications to species management and control, however, it is essential that controlling factors themselves are manageable. That imposes certain restrictions. For instance, the impact of environmental borders is very effective in blocking species spread (Keitt et al. 2001); however, it is hardly possible to use it as a practical tool for invasive species control. One biological factor that can be relatively easily managed and, at the same time, affects exotic species spread is predation. A decrease in the

invasion/colonization rates resulting from an increase in predation have been observed in field observations (Fagan and Bishop 2000). Later theoretical studies indicated that the impact of predation can block or reverse species invasion provided that the invasive species is affected by the Allee effect (Owen and Lewis 2001; Petrovskii et al. 2005a). As another example, a similar controlling strategy based on a deliberate introduction of a specialist predator has been also discussed in connection with the invasion of *Mnemiopsis leidyi* in the Black Sea ecosystem (Vinogradov et al. 1989). Introduction of *Beroe ovata*, which finally took place unintentionally a few years ago has indeed appeared to be very effective and nearly brought the population of *Mnemiopsis* to extinction (Vinogradov et al. 2000).

Another relevant factor that may significantly affect the spread of invasive species is the influence of infectious diseases. Although no detailed theoretical study of the impact of infection on the rates of spread has as yet been published, there are a few practical examples of infectious diseases being used successfully to control an invasion of exotic species, cf. (Fitzgerald and Veitch 1985; Courchamp and Sugihara 1999). There is growing evidence that viral infection can be just as important for aquatic species as for terrestrial ones; in particular, it might accelerate the termination of phytoplankton blooms (Tarutani et al. 2000; Jacquet et al. 2002; Gastrich et al. 2004). However, not much is yet known about marine viruses and their role in aquatic ecosystems and the species that they infect; some information along with a list of further references can be obtained from reviews by Fuhrman (1999), Suttle (2000) and Wommack and Colwell (2000).

Despite considerable recent progress, the impact of the above factors is still not studied well enough. Predation and/or infectious diseases affect invasion rates but they can also change the whole pattern of spread. It was shown that, as a result of the interplay between predation and the Allee effect, the usual invasion scenario when invasive species spreads over space through propagation of a population wave can change to a curious regime of patchy invasion (Petrovskii et al. 2002a, b). In this regime, no continuous travelling front is formed and the species invade via irregular motion and interaction of separate population patches. Note that this scenario of species spread is often observed in nature; however, its origin has not been fully understood so that different authors ascribe it to different mechanisms, such as environmental heterogeneity (Murray 1989), environmental stochasticity (Lewis 2000; Lewis and Pacala 2000), etc.

It is likely that this qualitative change in the pattern of spread from propagation of continuous travelling wave to patchy invasion has significant ecological implications. Hitherto, however, these implications have not been investigated in detail. In particular, it is still unclear whether the patchy invasion should be linked to a specific ecological interaction, such as predation, or is a more general phenomenon. In this paper we consider the patchy invasion arising in the problem of biological control using a few mathematical models of population dynamics and epidemiology. We first study a separate effect of predation (cf. Section 2) and infection (Sections 3 and 4) using simple deterministic models. By means of extensive computer simulations we show that invasive species can exhibit deterministic patchy invasion as a result of increasing pressure from predatory species or infectious disease. The patchy spread corresponds to the 'invasion at the edge of extinction' so that a small variation of parameters either restores the usual scenario of invasion via travelling population waves or brings the species to extinction. We also show that the system's dimensionality is essential: for the parameter values when the patchy invasion is observed in the model with two spatial dimensions, the species goes extinct in the corresponding 1-D case. We then proceed to a more realistic case, in Section 5, considering the joint effect of predation and infection and also taking into account environmental noise. Using a model of a marine food chain as an example, we show that, under the impact of noise, the patchy spread can also be observed in a system without Allee effect.

Patchy invasion in a predator–prey system: a paradigm

In order to study the impact of predation on the spread of invasive species, we consider the

spatiotemporal dynamics of a predator–prey system described by the following equations:

$$\frac{\partial U(\mathbf{r},T)}{\partial T} = D_1\nabla^2 U(\mathbf{r},T) + P(U) - E(U,V), \tag{1}$$

$$\frac{\partial V(\mathbf{r},T)}{\partial T} = D_2\nabla^2 V(\mathbf{r},T) + \kappa E(U,V) - MV \tag{2}$$

(Nisbet and Gurney 1982; Murray 1989; Holmes et al. 1994; Shigesada and Kawasaki 1997) where $U(\mathbf{r},t)$ and $V(\mathbf{r},t)$ are the concentrations of prey and predator, respectively, $\mathbf{r}=(X,Y)$ is the position in space, T is the time, D_1 and D_2 are the diffusivities of prey and predator, respectively. Function $P(U)$ describes the local prey growth whereas $E(U,V)$ describes predation; M is the mortality rate of the predator and κ the coefficient of food utilization.

The particular choice of the functions $P(U)$ and $E(U,V)$ in Equations (1–2) may vary, depending on the properties of particular species. In this paper we assume that the local growth of the prey is damped by the Allee effect:

$$P(U) = \left(\frac{4\eta}{(K-U_0)^2}\right)U(U-U_0)(K-U) \tag{3}$$

(cf. Lewis and Kareiva 1993) where K is the prey carrying capacity and η is the maximum *per capita* growth rate. Here U_0 can be considered as a measure of the intensity of the Allee effect: the lower the value of U_0, the less prominent is the Allee effect. The Allee effect is called 'strong' when $0<U_0<K$; in this case U_0 has the meaning of a 'threshold' so that for $U<U_0$ the growth rate becomes negative. For $-K<U_0\leq 0$, the Allee effect is called 'weak', and for $U_0\leq -K$ the Allee effect is absent.

For the predator, we assume that it shows the Holling type II trophical response:

$$E(U,V) = \frac{AUV}{U+B} \tag{4}$$

where A describes predation intensity and B is the half-saturation prey density.

From (1–4), we arrive at the following system:

$$\frac{\partial U(\mathbf{r},T)}{\partial T} = D_1\nabla^2 U(\mathbf{r},T) + \left(\frac{4\eta}{(K-U_0)^2}\right)U(U-U_0)(K-U) - \frac{AUV}{U+B}, \tag{5}$$

$$\frac{\partial V(\mathbf{r},T)}{\partial T} = D_2\nabla^2 V(\mathbf{r},T) + \kappa\frac{AUV}{U+B} - MV. \tag{6}$$

For convenience of numerical simulations and also in order to decrease the number of parameters, we introduce dimensionless variables: $u=U/K$, $v=V/(\kappa\ K)$, $x=X(a/D_1)^{1/2}$, $y=Y(a/D_1)^{1/2}$ and $t=aT$ where $a=A\kappa K/B$. Then, from Equations (5–6), we obtain:

$$\frac{\partial u(x,y,t)}{\partial t} = \left(\frac{\partial^2 u}{\partial x^2}+\frac{\partial^2 u}{\partial y^2}\right) + \beta u(u-b)(1-u) - \frac{uv}{1+\Lambda u}, \tag{7}$$

$$\frac{\partial v(x,y,t)}{\partial t} = \epsilon\left(\frac{\partial^2 v}{\partial x^2}+\frac{\partial^2 v}{\partial y^2}\right) + \frac{uv}{1+\Lambda u} - mv \tag{8}$$

where $\Lambda=K/B$, $b=U_0/K$, $\beta=4\eta BK/(A\kappa(K-U_0)^2)$, $m=M/a$ and $\epsilon=D_2/D_1$.

Invasion of exotic species usually starts with species introduction when a number of individuals of given species are brought locally into a new ecosystem. It means that the initial condition for Equation (7) is most naturally described by a function of compact support. In particular, in our numerical simulations we used the following initial condition:

$$u(x,y,0)=u_0 \text{ if } x_{11}<x<x_{12} \text{ and } y_{11}<y<y_{12}, \text{ otherwise } u(x,y,0)=0 \tag{9}$$

where u_0 is the initial prey density and parameters x_{11}, x_{12}, y_{11}, y_{12} define the size of the infested domain.

The idea to use predation as a 'tool' in order to slow down or block the spread of invasive species implies that, soon enough after introduction of given exotic species, a small population of a relevant predatory species is introduced locally into the region already inhabited by its prey. Thus, the corresponding initial condition for Equation (8) is as follows:

$$v(x,y,0) = v_0 \text{ if } x_{21} < x < x_{22} \text{ and } y_{21} < y < y_{22},$$
$$\text{otherwise } v(x,y,0) = 0 \tag{10}$$

where v_0 is the initial predator density and x_{21}, x_{22}, y_{21}, y_{22} are parameters with obvious meaning.

Petrovskii et al. (2002a, b) have shown that, for certain parameter values, the species spread described by (7–8) takes place via an unusual scenario: the evolution of initial conditions (9–10) leads not to formation of the intuitively expected continuous circular front but to a curiously shaped, patchy structure. The species invasion then takes place not due to the expansion of the circular front but due to irregular motion and interaction of separate patches. It was also shown that this phenomenon of patchy invasion is an essential consequence of the strong Allee effect and that it takes place for various parameter sets, although different parameters cannot vary independently. However, the origin of the phenomenon and its implications for population dynamics remained obscure.

Now, in order to gain a deeper insight into the phenomenon of patchy invasion, along with system (7–8) we consider its one-dimensional reduction, i.e.,

$$\frac{\partial u(x,t)}{\partial t} = \frac{\partial^2 u}{\partial x^2} + \beta u(u-b)(1-u) - \frac{uv}{1+\Lambda u}, \tag{11}$$

$$\frac{\partial v(x,t)}{\partial t} = \epsilon \frac{\partial^2 v}{\partial x^2} + \frac{uv}{1+\Lambda u} - mv. \tag{12}$$

Similarly to the 2-D case, the initial species distribution in the 1-D case is considered as follows:

$$u(x,0) = u_0 \text{ for } -\Delta_u < x < \Delta_u, \quad \text{otherwise } u(x,0) = 0, \tag{13}$$

$$v(x,0) = v_0 \text{ for } -\Delta_v < x < \Delta_v, \quad \text{otherwise } v(x,0) = 0 \tag{14}$$

where Δ_u and Δ_v give the radius of the initially invaded domain.

It should be mentioned here that one essential property of the system with the Allee effect for prey is that, for any parameter value, there exist initial conditions that lead to species extinction. In general, these are the conditions with sufficiently small diameter of initially inhabited domain and/or sufficiently small value of the initial prey density. For instance, it can readily be seen that, in the case that max $u(x,y,0) < b$, the species go extinct independently of the other parameter values. To avoid ambiguity, throughout this paper we always chose a large enough initial prey density and/or initial diameter.

Equations (7–8) and (11–12) were solved numerically by finite differences for a wide range of parameters. In most cases we used the simple explicit scheme; however, to avoid numerical artifacts, some of the results were reproduced using more advanced approaches. In particular, for the 1-D system (11–12), an implicit scheme with the built-in sweeping method was also used, and for the 2-D system we used an alternate directions method. Moreover, the sensitivity of the results to the choice of the mesh steps was checked and the steps have been chosen to be sufficiently small. The results shown below were obtained for $\Delta t = 0.1$, $\Delta x = \Delta y = 1$ for the 2-D problem and for $\Delta t = 0.1$, $\Delta x = 0.5$ for the 1-D problem.

In both 1-D and 2-D cases, the Neumann 'no-flux' conditions are placed at the boundary of the numerical domain. The size of the domain is chosen large enough so that, during the simulation time, the impact of the boundaries has been kept as small as possible.

In order to reveal the succession of the regimes of the system dynamics in response to parameter changes, we choose predator mortality m as a controlling parameter and keep all other parameters fixed at certain hypothetical values. Specifically, we consider the following set of parameters: $\Lambda = 0.1$, $b = 0.2$ and $\beta = 2$.

It is well-known that, for values of m not too small, the 1-D system (11–12) demonstrates a variety of travelling population fronts, see (Murray 1989; Sherratt et al. 1995; Petrovskii and Malchow 2000; Sherratt 2001; Petrovskii et al. 2005b) for examples and details, and (Volpert et al. 1994) for a more rigorous consideration. The propagating front can be followed either by a stationary spatially homogeneous species distribution or by irregular spatiotemporal patterns. The regimes in the corresponding 2-D system arise as an immediate generalization of the

regimes observed in the 1-D case. For instance, instead of two travelling fronts running from the place of the species introduction (described by the initial conditions of compact support), in the 2-D system the species spread via an expanding circular front.

However, the situation changes significantly when m becomes small enough, a case which corresponds to a 'stronger' predator and thus to more intense predation. In this case, in the 1-D system the invasive species spreads not through propagation of population fronts but rather through motion of separate patches or groups of patches. Figure 1 shows the snapshots of the population density obtained for $m=0.418$ and the initial conditions (13–14) with $\Delta_u=100$, $\Delta_v=20$, $u_0=1.0$, $v_0=0.2$. Since the problem is symmetrical with respect to $x\to -x$, only one half of the numerical domain is shown. Remarkably, for the same parameter values, the species spread in two spatial dimensions still takes place through an expanding front of perfectly circular shape: Figure 2 shows the 2-D snapshots of the prey density obtained for the initial conditions

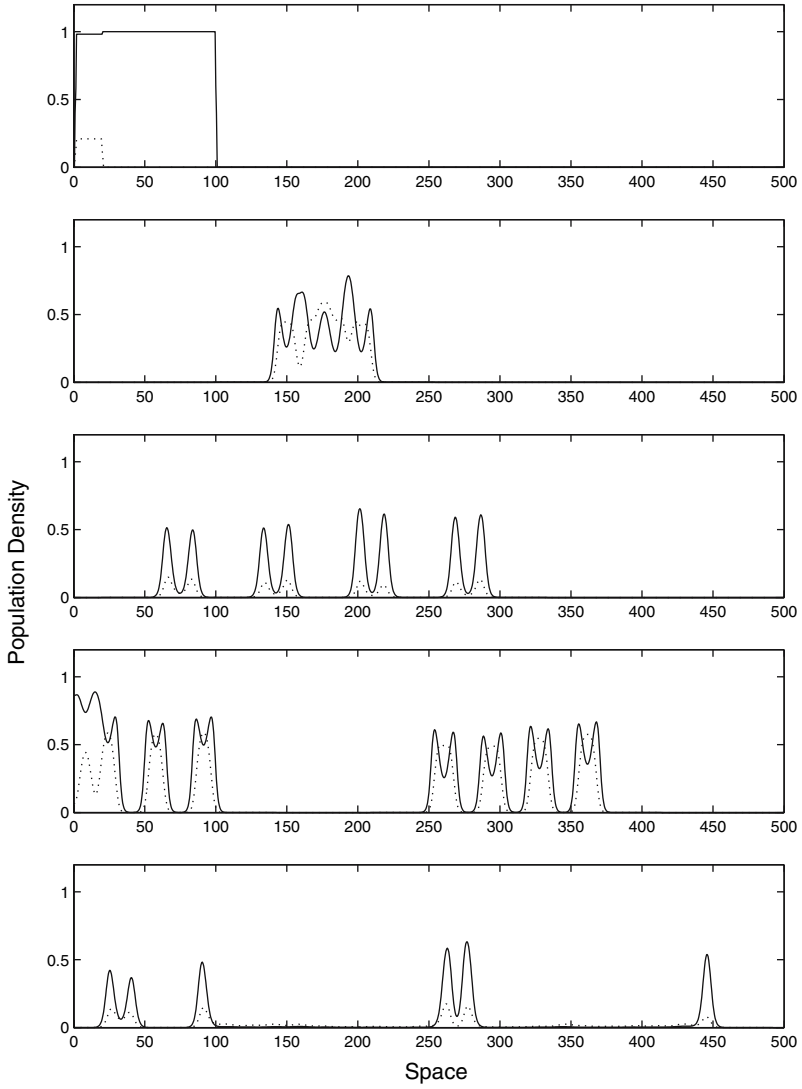

Figure 1. 1D density of prey (solid curve) and predator (dotted curve) calculated at equidistant moments with $\Delta t=250$ for parameters $\epsilon=1$, $\Lambda=0.1$, $b=0.2$, $\beta=2$, $m=0.418$.

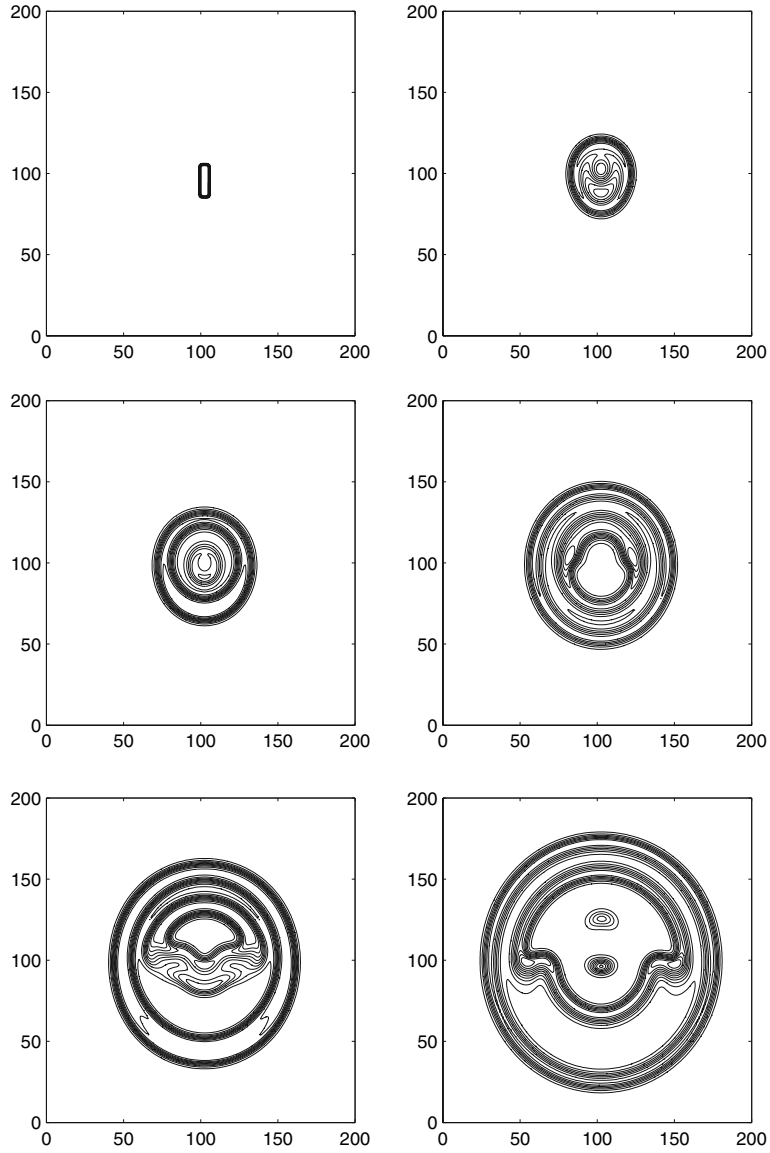

Figure 2. Isoclines of prey density (predator density exhibits similar properties) calculated at equidistant moments with $\Delta t = 40$ for parameters of Figure 1. Thick lines correspond to regions with large density gradient and thus show the patch boundary.

(9–10) with $x_{11} = 85$, $x_{12} = 105$, $x_{21} = 85$, $x_{22} = 95$, $y_{11} = 100$, $y_{12} = 105$, $y_{21} = 95$, $y_{22} = 115$ and $u_0 = 1.0$, $v_0 = 0.2$.

A further decrease in m results in species extinction in the 1-D system. That has a clear biological implication: the predator becomes strong enough, it catches up with the spreading prey and brings it down. Figure 3 shows the 1-D snapshots of the population density obtained for $m = 0.410$ and the same initial conditions as in Figure 1.

Surprisingly, for the same parameter values, the system dynamics in two spatial dimensions does not lead to species extinction, see Figure 4 (obtained for the same initial conditions as Figure 3). The species invasion still takes place, but not through the expanding continuous circular front as in the previous case. Instead, at any moment of time, the invaded area has an irregular shape and can even split into disconnected patches. A further decrease in m leads to species

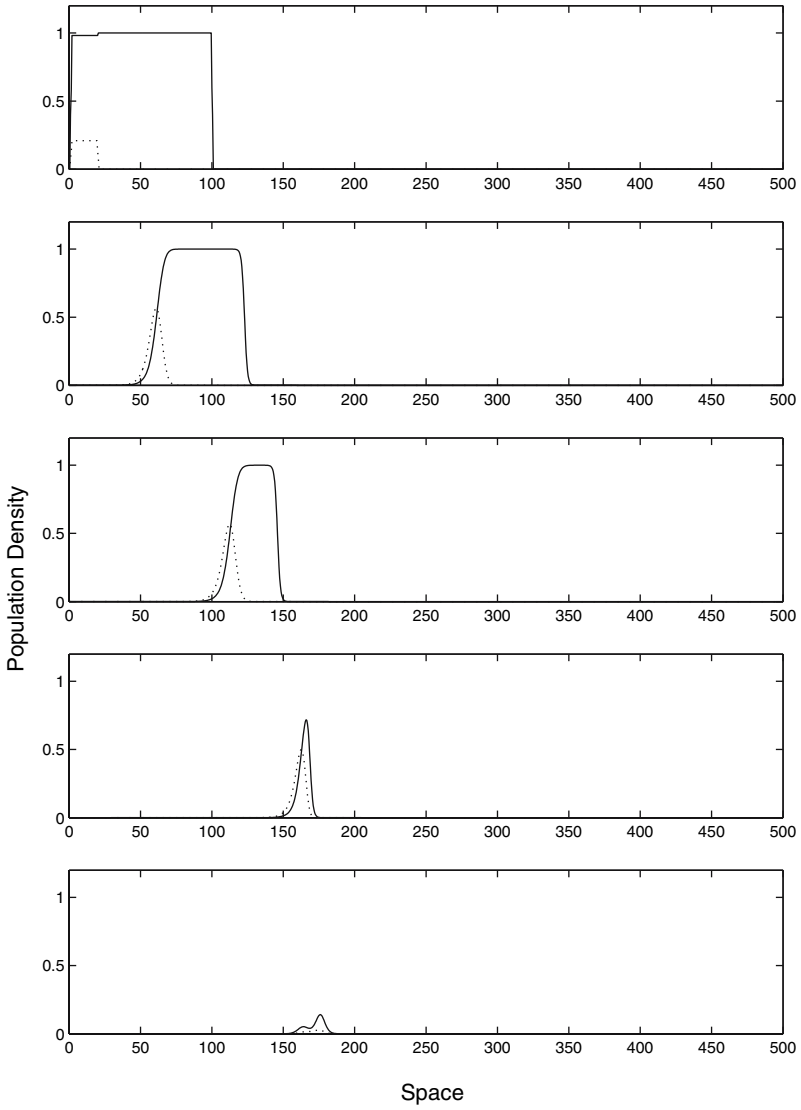

Figure 3. 1D density of prey (solid curve) and predator (dotted curve) calculated at equidistant moments with $\Delta t = 39$ for $m = 0.410$. Other parameters are as in Figure 1.

extinction in the 2-D system, just as it happened in the 1-D system for a somewhat larger value of m.

Note that, in the system (7–8), there is no prescribed spatial heterogeneity (e.g. via coefficients dependent on space) and the irregularity of the pattern shown in Figure 4 is self-organized. A closer inspection shows that the system dynamics corresponding to the patchy invasion can be qualified as spatiotemporal chaos (Petrovskii et al. 2002a; Morozov et al. 2004). This may account for the apparent asymmetry of the spatial patterns observed for large times, cf. the bottom of Figure 4: since chaos means an intrinsic instability of the system dynamics, a small perturbation due to numerical approximation error finally results in a considerable discrepancy between the species distibution in the left-hand and right-hand parts of the domain.

We want to emphasize that the parameters of Figure 4 are not at all unique, and a qualitatively similar pattern of species spread can be observed for other parameter values as well. We do not

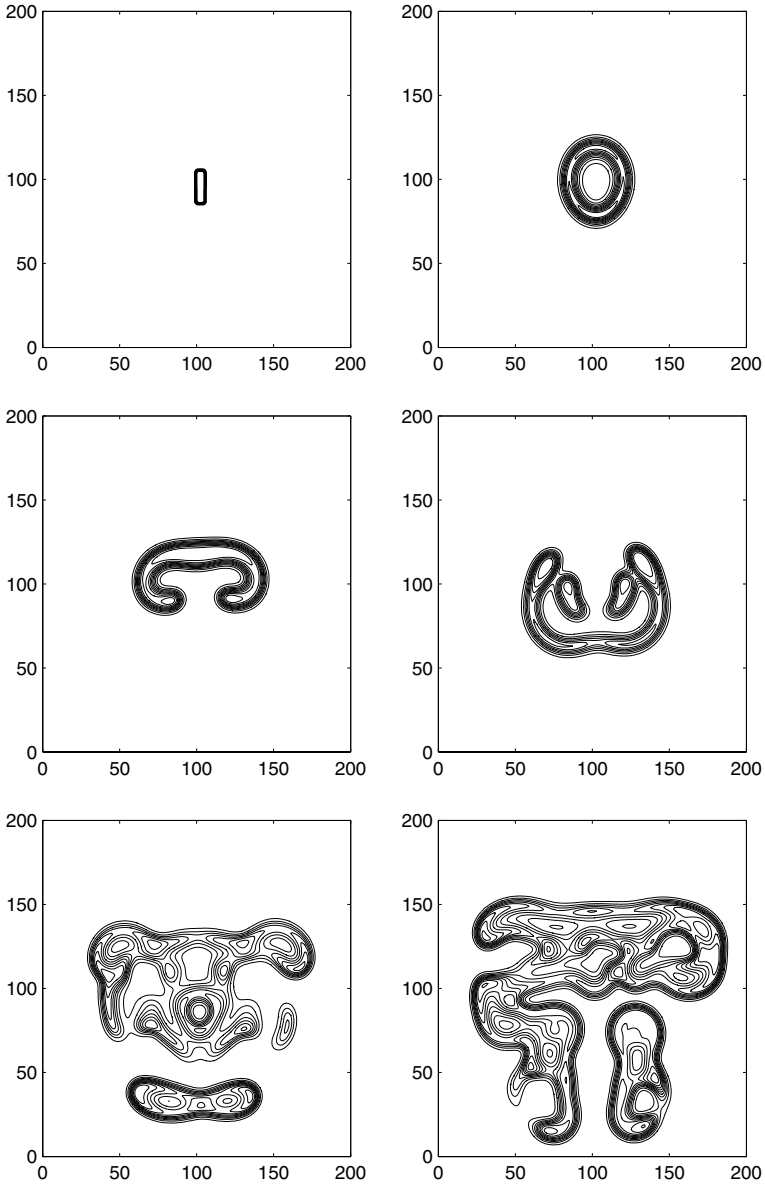

Figure 4. 2-D density of prey (predator density exhibits similar properties) calculated at the moments $t=0$; $t=50$; $t=150$; $t=250$; $t=350$; $t=400$ (from left to right, from top to bottom) for parameters of Figure 3.

show other examples for the sake of brevity. For Λ, b and β fixed as above, the regime of patchy spread can be observed for the values of m from a short range situated around $m=0.418$. For other values of Λ, b and β, the regime of patchy invasion can be observed for different m. Moreover, similar effects are observed if we choose another controlling parameter, e.g. the threshold density b, and keep other parameters fixed. In this case, an increase in b (instead of a decrease in m) eventually leads from species invasion through propagation of continuous fronts to patchy invasion. Comparative analysis of the simulation results shows that the regime of patchy invasion in the 2-D model always happens 'at the edge of extinction' so that a further small change of the controlling parameter, i.e., either m or b, leads to species extinction in two dimensions too.

The succession of regimes of the system dynamics is outlined in Figure 5. A remarkable and surprising feature of the patchy spread is that the dynamics of the corresponding 1-D model for the same parameters leads to species extinction, cf. Figures 3 and 4.

SI model of epidemic disease

Another possibility of biological control of invasive species is related to the impact of infectious diseases. In order to address this issue, we start with one of the simplest models of epidemiology, namely, with the so-called SI model:

$$\frac{\partial S(\mathbf{r},t)}{\partial t} = \left(\frac{\partial^2 S}{\partial x^2} + \frac{\partial^2 S}{\partial y^2}\right) + \beta S(S-b)(1-S) - SI, \tag{15}$$

$$\frac{\partial I(\mathbf{r},t)}{\partial t} = \epsilon\left(\frac{\partial^2 I}{\partial x^2} + \frac{\partial^2 I}{\partial y^2}\right) + SI - mI \tag{16}$$

(Murray 1989) where S and I are the densities of the susceptible and infected individuals, respectively, at moment t and position $\mathbf{r}=(x,y)$. Correspondingly, $S+I$ gives the total population density of given invasive species. The term SI describes the disease transmission rate from infected to susceptible individuals. We consider the case when the disease is sufficiently serious that infected individuals cannot produce offspring and the population can grow only due to multiplication of susceptibles. For the sake of brevity, we assume that in Equations (15–16) all variables are already scaled to dimensionless values. As above, along with 2-D SI model, we consider its one-dimensional analogue; the corresponding equations are not shown for the sake of brevity.

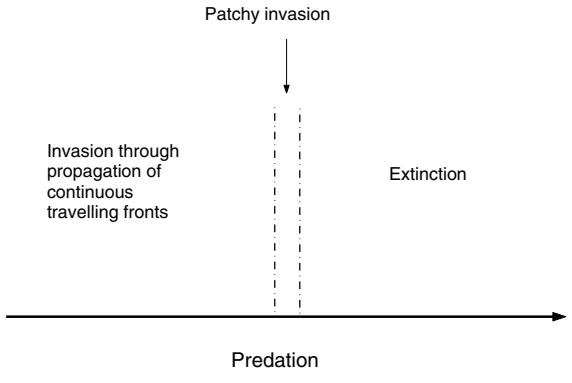

Figure 5. Invasion at the edge of extinction: sketch of system dynamics.

Note that, from the mathematical aspect, the system (15–16) is not just a particular case of Equations (7–8) corresponding to $\Lambda=0$. The decrease from $\Lambda>0$ to $\Lambda=0$ corresponds to a certain structural change: instead of strong nonlinearity $uv/(1+\Lambda u)$, we now have a bilinear term which corresponds to the classical Lotka–Volterra model. It is well-known that the dynamics of the model with bilinear interaction term and with Holling type II can differ in many aspects, cf. (Murray 1989).

According to the corresponding idea of biological control, in order to prevent the spread of a harmful species, at an early stage of invasion a number of individuals are deliberately infected by a certain lethal disease, cf. (Courchamp and Sugihara 1999; Fitzgerald and Veitch 1985). Thus, the initial conditions in the form (9–10) for 2-D system and (13–14) for 1-D system are still appropriate, with the appropriate change of notation.

The system (15–16) has been thoroughly studied by means of numerical simulations. We find that the succession of the regimes in response to a change in a controlling parameter, either m or b, is similar to the ones observed for the predator–prey system. In the 1-D system, a decrease in m first changes the pattern of disease spread via propagation of travelling fronts to motion of separate patches. In two spatial dimensions, however, it still corresponds to the disease spreading via expansion of a continuous front of perfectly circular shape. A further decrease in m fully eradicates the species in the 1-D model but leads to its patchy spread in two dimensions. For smaller m the species goes extinct. Thus, again, the patchy spread gives a scenario of species/infection spread at the edge of extinction. For the sake of brevity, we do not show the corresponding figures here; details can be found in (Petrovskii and Venturino 2004).

Note that, although the succession of dynamical regimes described above when a decrease in

m eventually leads to species extinction may seem to be somewhat counter-intuitive, it is in full agreement with biological arguments. Indeed, the dimensionless parameter m gives, up to a certain factor, a ratio of the infected mortality rate and the transmission rate. A decrease in m thus corresponds to an increase in the transmission rate which tends to make disease more dangerous.

Patchy spread in SIR model

In the previous section, we have shown that the regime of patchy spread of invasive species can arise in response to controlling efforts based on the introduction of a certain infectious disease. The patchy invasion in this case has exactly the same implication as in the predator–prey system: it describes the scenario of spatial spread at the edge of extinction so that a further small change of the controlling parameter leads to species extinction. As well as in the case of the predator–prey model, for the parameters when the patchy spread takes place in two spatial dimensions, in the 1-D model the species goes extinct.

The results of the previous section inspire us to look now at the dynamics of a more complicated epidemiological model. In this section we consider the spatiotemporal dynamics of an infectious disease described by the following equations:

$$\frac{\partial S(\mathbf{r},t)}{\partial t} = \left(\frac{\partial^2 S}{\partial x^2} + \frac{\partial^2 S}{\partial y^2}\right) + \beta u(S-b)(1-S) - SI + \alpha I + \delta R, \tag{17}$$

$$\frac{\partial I(\mathbf{r},t)}{\partial t} = \left(\frac{\partial^2 I}{\partial x^2} + \frac{\partial^2 I}{\partial y^2}\right) + SI - mI - \alpha I - \sigma I, \tag{18}$$

$$\frac{\partial R(\mathbf{r},t)}{\partial t} = \epsilon\left(\frac{\partial^2 R}{\partial x^2} + \frac{\partial^2 R}{\partial y^2}\right) + \sigma I - \delta R - \omega R \tag{19}$$

(so-called SIR model) where S is the density of the susceptible individuals of given population, I is the density of infected and R is the density of removed individuals at the position $\mathbf{r}=(x,y)$ and time t. Equations (17–19) are already scaled to dimensionless values. As in the case of the SI model, we assume that only the susceptibles can produce offspring.

Obviously, the SIR model is more complicated than the SI model and contains many more mechanisms and scenarios of disease development. Moreover, it allows a somewhat different biological interpretation. For instance, R can be treated as the density of individuals that recovered from the disease but cannot become susceptible again, e.g., because they become immunized. In this case, I gives the density of sick individuals. Alternatively, R can be treated as the density of sick individuals; in this case I gives the density of the individuals who have the disease in the latent stage. More details and further references can be found in (Diekmann and Heesterbeek 2000; Hethcote 2000).

Typical results of computer simulations using the SIR model are shown in Figures 6–11. We use the initial conditions of the same type as given by (9–10) (with obvious change of notation) and assume that at the beginning of the disease spread the removed subpopulation is absent, i.e., $R(x,y,0)=0$. As above, along with the 2-D system (17–19) we consider its 1-D reduction. In that case, the initial conditions for S and I are given by (13–14).

Since the SIR model has additional feedbacks, e.g. through possible recovery of the removed individuals, cf. the last terms in Equations (17) and (19), the system response to variation of the mortality m of infected is somewhat more complicated than it is in the SI model. For that reason, in our search for the regime of patchy spread, it appears more convenient to vary b, not m, and to keep all other parameters fixed. For numerical simulations, we chose the following hypothetical values: $\epsilon=0.5$, $\alpha=0$, $\beta=4$, $\delta=0.1$, $m=0$, $\omega=0.8$, $\sigma=0.5$. In our choice of parameter values we are more inclined to consider R as the density of sick subpopulation and I as the latent subpopulation, which is why we neglect the mortality rate of infected individuals and choose $\epsilon<1$. We ought to mention, though, that the assumption $m=0$ is not a principal restriction. While large values of m can indeed change the system properties significantly, for m positive but small the dynamics remains qualitatively the same as for $m=0$.

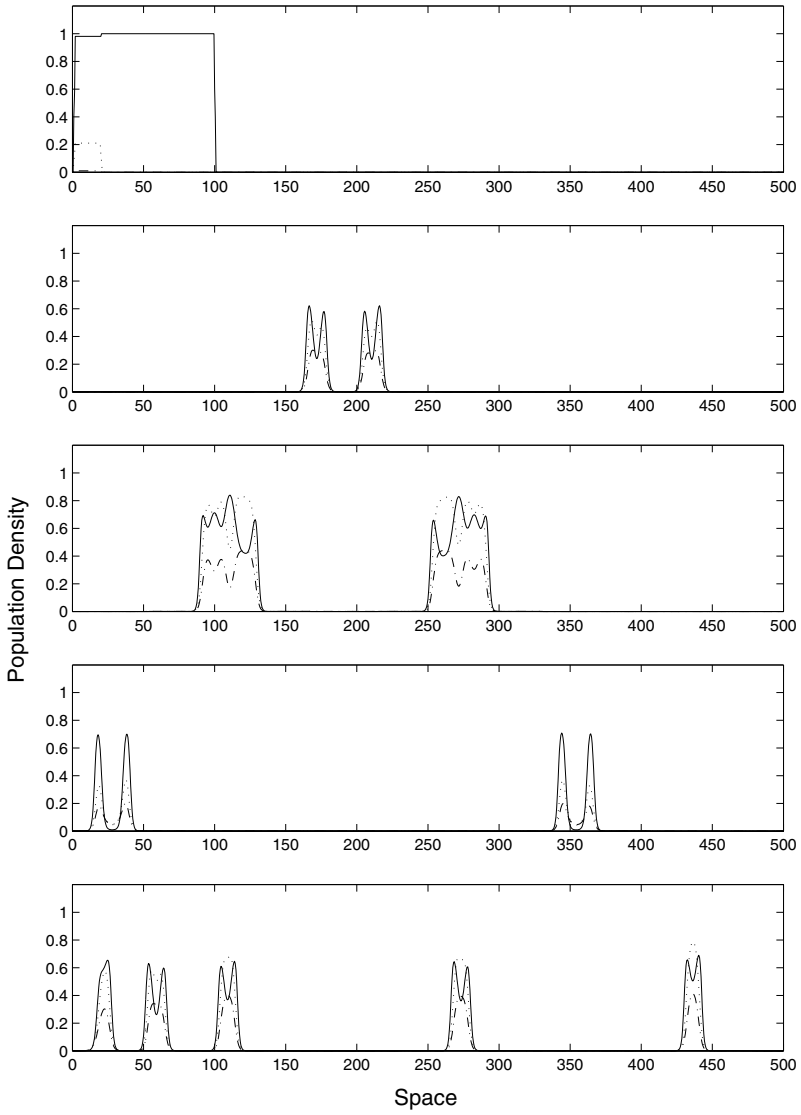

Figure 6. 1-D density of susceptibles (solid curve), infected (dotted curve) and removed (dashed-and-dotted line) calculated in the SIR model at equidistant moments with $\Delta t = 250$ for parameters $\epsilon = 0.5$, $b = 0.26$, $\alpha = 0$, $\beta = 4$, $\delta = 0.1$, $m = 0$, $\omega = 0.8$, $\sigma = 0.5$.

For the 1-D case the species spread from the place of original introduction occurs through propagation of a travelling population front, for sufficiently small values of b, in the same way as it takes place for the predator–prey and SI models considered above. The species distribution behind the front can be either homogeneous and stationary or patchy and transient, depending on b. In all those cases, the species spread in the corresponding 2-D system takes place through an expanding population front of circular shape. For somewhat larger b the regime of spread in 1-D system turns to propagation of separate patches, or groups of patches. Figure 6 shows the 1-D snapshots of the species density (solid curve for susceptibles, dashed for infected, dashed-and-dotted for removed) obtained for $b = 0.26$ (for the initial conditions $\Delta_S = 100$, $\Delta_I = 20$, $S_0 = 1.0$, $I_0 = 0.2$). Remarkably, for the same value of b the species spread in the 2-D system still takes place through an expanding circular front, see Figure 7 (for the initial conditions $x_{11} = 130$,

$x_{12}=155$, $x_{21}=130$, $x_{22}=145$, $y_{11}=145$, $y_{12}=165$, $y_{21}=145$, $y_{22}=160$, $S_0=1.0$, $I_0=0.2$).

A further increase in b leads to species extinction in the 1-D system, see Figure 8 obtained for $b=0.27$ and the same initial condition as in Figure 6. In the 2-D system, for the same parameter values, the evolution of the initial conditions does not lead to species extinction but to its spread, although the form of the front is no longer circular and continuous, see Figure 9. Larger values of b make the patchiness of the spatial pattern even more distinct, see Figures 10 and 11 obtained for $b=0.273$ and $b=0.274$, respectively. Furthermore, the rate of spread becomes much lower with an increase in b, cf. Figures 9 and 11. These results confirm our hypothesis that the regime of patchy spread provides a mechanism for the species to persist and even to invade at the edge of extinction.

Surprisingly, a further increase in b does not immediately lead to species extinction in two dimensions but first to formation (in the large time frame, asymptotic) of stationary patchy distribution of the species. Figure 12 shows the 2-D snapshots of the species density obtained for $b=0.275$. After the transient stage, which takes a considerable time, $t \simeq 1500$, a few stationary patches of the population density appear, see the bottom of Figure 12. Calculations performed for larger time confirm that the patches remain stationary.

We should to mention that the regime of formation of stationary patchy patterns in the SIR model can be observed for other parameter values too, although the number of patches can be different. For instance, for $b=0.276$, evolution of the same initial conditions as in Figures 9 to 12 lead to formation of only two stationary patches. In turn, the choice of the initial conditions can affect both the number of patches and their position.

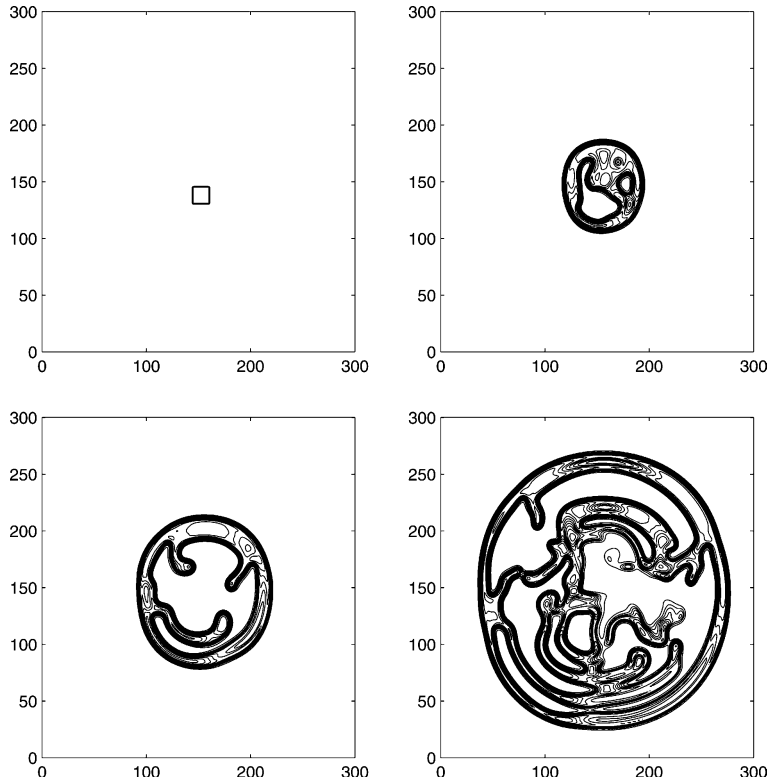

Figure 7. 2-D density of infected calculated in the SIR model at moments $t=0$; $t=100$; $t=200$; $t=400$ (from left to right, from top to bottom) for the same parameters as in Figure 6. Except for the very early stage of the system dynamics, the density of susceptibles and removed exhibits similar properties.

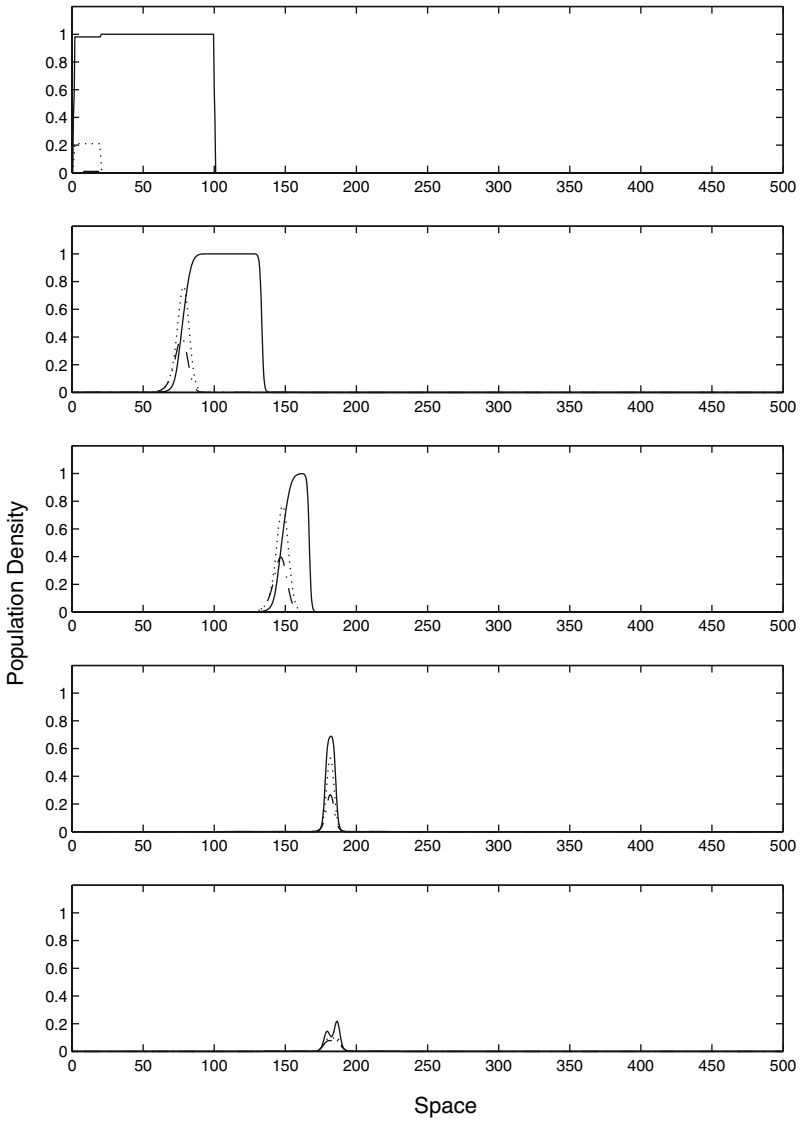

Figure 8. 1-D density of susceptibles (solid curve), infected (dotted curve) and removed (dashed-and-dotted line) calculated in the SIR model at equidistant moments with $\Delta t = 52.5$ for $b = 0.27$. Other parameters are as in Figure 6.

Patchy spread in a stochastic model of virally infected phytoplankton and zooplankton

Mathematical models of the dynamics of virally infected phytoplankton populations are relatively rare. The by now classic publication is by Beltrami and Carroll (1994); a more recent work is that of Chattopadhyay and Pal (2002) and Chattopadhyay et al. (2003). The latter papers deal with lytic infections and mass action incidence functions (Nold 1980; Dietz and Schenzle 1985; McCallum et al. 2001). Meanwhile, the role of lysogeny remains largely obscure. While a lytic infection leads to the loss of reproduction and eventual destruction of the host cell, a lysogenic infection implies a certain strategy: the viruses integrate their genome into the host's genome so that reproduction of the host also results in virus reproduction (Jiang and Paul 1998; Ortmann et al. 2002).

The spatial aspect of infected populations has also been investigated relatively infrequently. Much has been published about the spatiotemporal

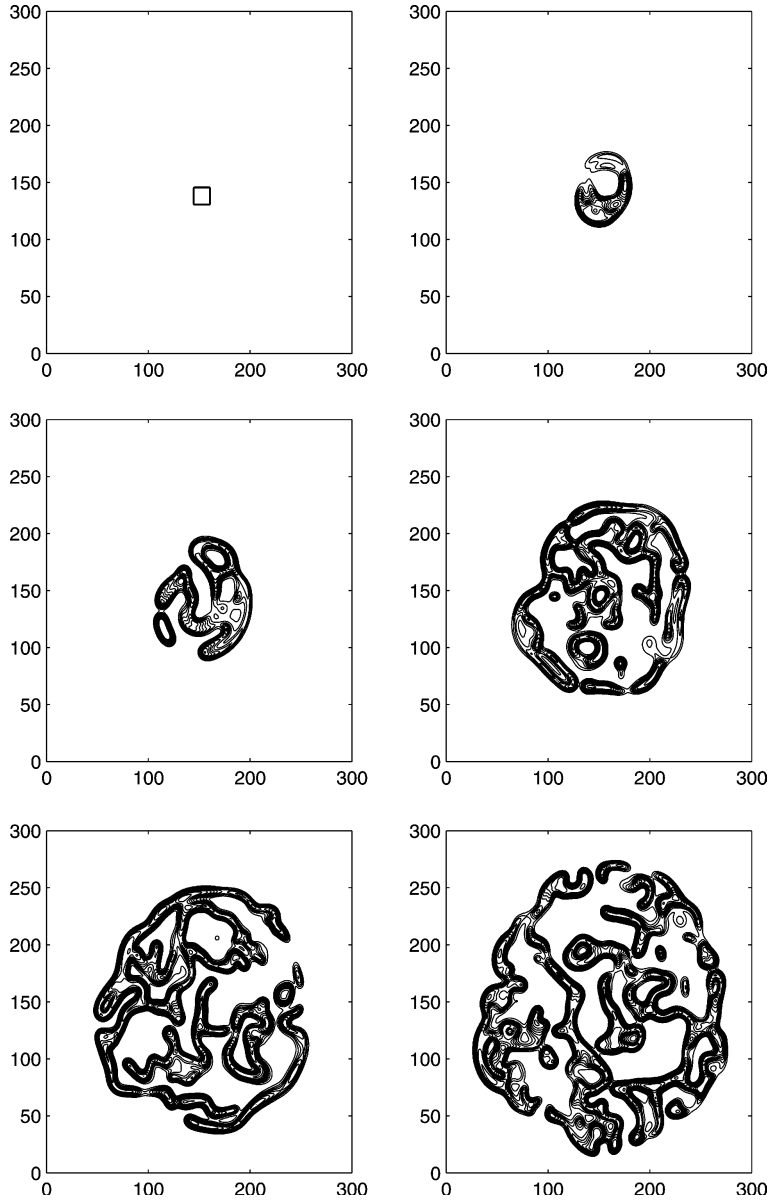

Figure 9. 2-D density of infected calculated in the SIR model at the moments $t=0$; $t=100$; $t=200$; $t=400$; $t=500$; $t=600$ (from left to right, from top to bottom) for the same parameters as in Figure 8.

self-organization in prey–predator communities, modelled by reaction-diffusion(-advection) equations, cf. (Medvinsky et al. 2002) for an extensive list of references. Much less is known about equation-based modelling of the spatial spread of epidemics; a small collection of papers includes Grenfell et al. (2001), Abramson et al. (2003), Lin et al. (2003) and Zhdanov (2003).

In this section, the focus is on modelling the influence of lysogenic infections and proportionate mixing incidence function (frequency-dependent transmission) on the spatial spread of interacting phytoplankton and zooplankton. The impact of multiplicative noise (Allen 2003; Anishenko et al. 2003) is considered as well in order to make the model more realistic.

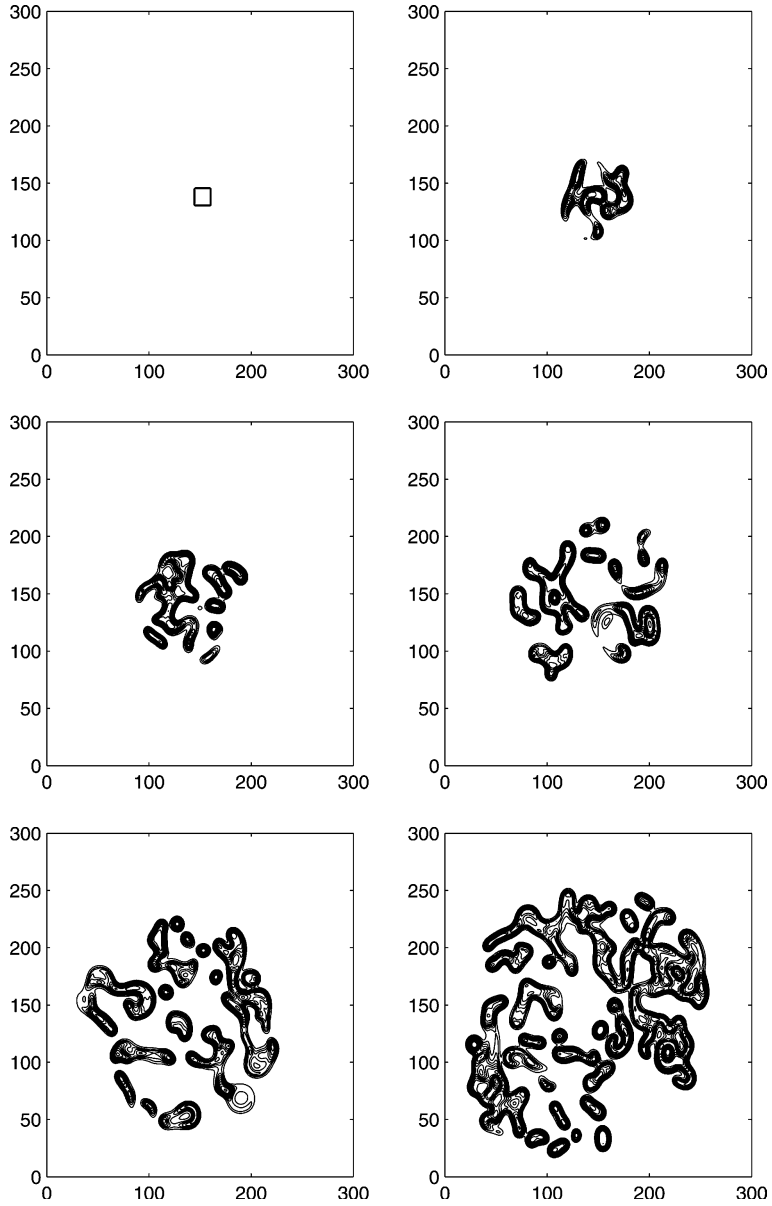

Figure 10. 2-D density of infected calculated in the SIR model at the moments $t=0$; $t=200$; $t=400$; $t=700$; $t=1000$; $t=1300$ (from left to right, from top to bottom) for $b=0.273$. Other parameters are as in Figures 8 and 9.

The model by Scheffer (1991) for the prey–predator dynamics of phytoplankton u and zooplankton v is used as the starting point. It reads in time t and two spatial dimensions $\mathbf{r}=(x, y)$ with dimensionless quantities, scaled following Pascual (1993)

$$\frac{\partial u}{\partial t} = \gamma u(1-u) - \frac{auv}{1+bu} + d\nabla^2 u, \tag{20}$$

$$\frac{\partial v}{\partial t} = \frac{auv}{1+bu} - m_3 v + d\nabla^2 v. \tag{21}$$

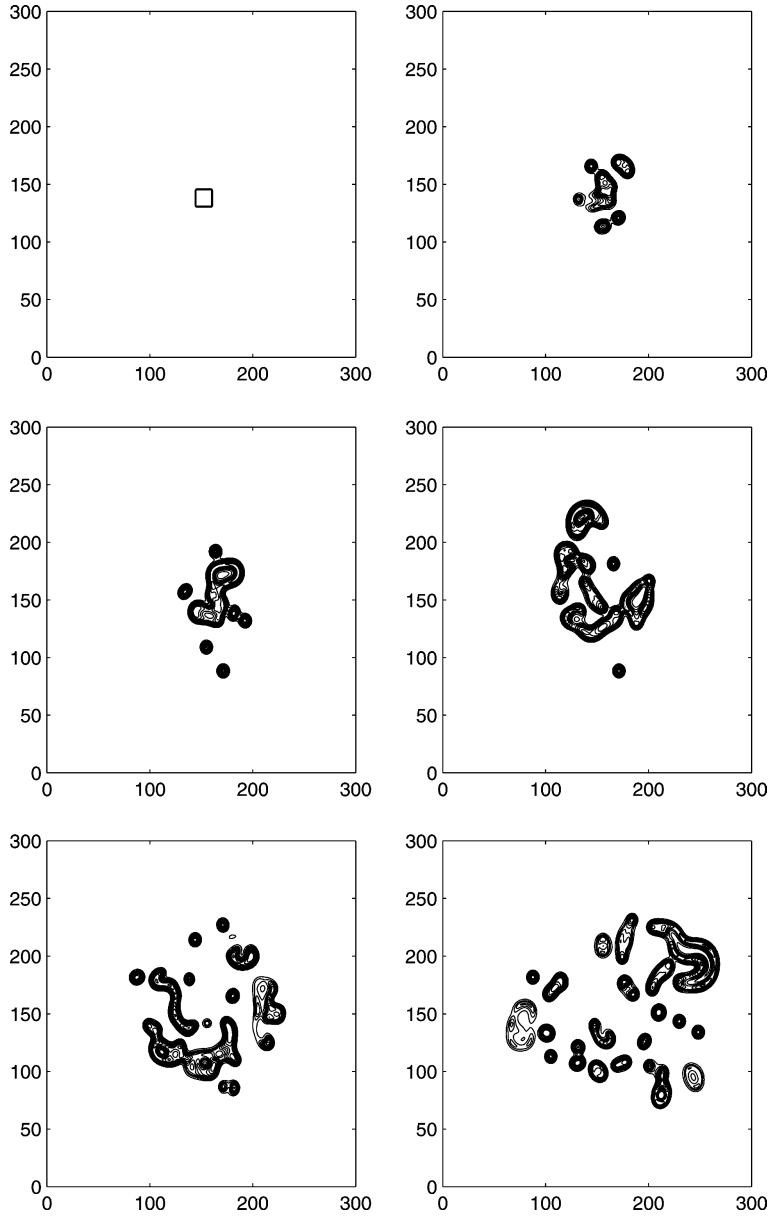

Figure 11. 2-D density of infected calculated in the SIR model at equidistant moments with $\Delta t = 500$ (from left to right, from top to bottom) for $b = 0.274$. Other parameters are as in Figures 8–10.

Here the phytoplankton grows logistically with intrinsic rate γ and Holling-type II grazing with maximum rate a; the zooplankton has a natural mortality with rate m_3. The growth rate γ is scaled as the ratio of local rate γ_{loc} and spatial mean $<\gamma>$. The dimensionless diffusion coefficient d describes eddy diffusivity: it must therefore be equal for both species. The dynamics of a top predator, i.e., planktivorous fish, is neglected because the focus is on the influence of virally infected phytoplankton.

The phytoplankton population u is split into a susceptible part u_1 and an infected portion u_2. Zooplankton is renamed u_3 in order to attain symmetry in notation. Then, the model system for symmetric inter- and intraspecific competition of susceptibles and infected reads

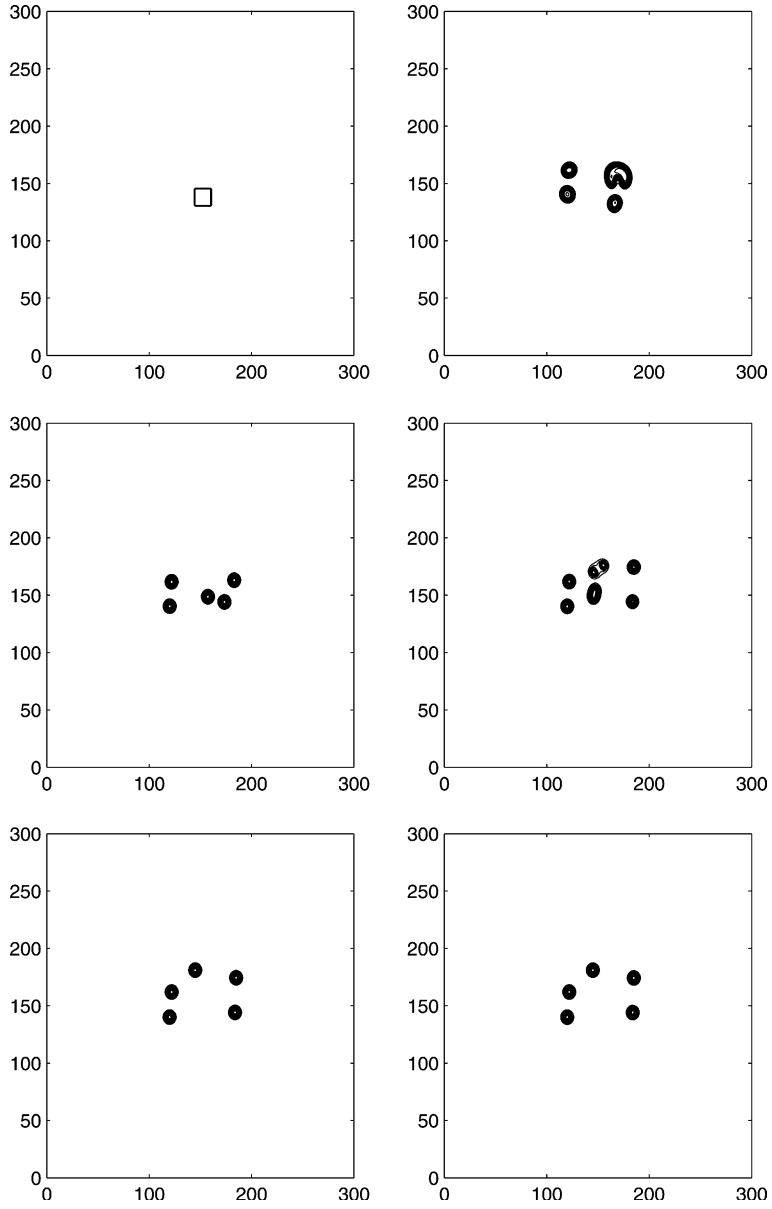

Figure 12. 2-D density of infected calculated in the SIR model at equidistant moments with $\Delta t = 500$ (from left to right, from top to bottom) for $b = 0.275$. Other parameters are as in Figures 8–11.

$$\frac{\partial u_i(\mathbf{r},t)}{\partial t} = f_i[\mathbf{u}(\mathbf{r},t)] + d\nabla^2 u_i(\mathbf{r},t), i = 1,2,3; \quad (22)$$

where

$$f_1 = \gamma_1 u_1(1-u_1-u_2) - \frac{a u_1 u_3}{1+b(u_1+u_2)} - \lambda \frac{u_1 u_2}{u_1+u_2}, \quad (22a)$$

$$f_2 = \gamma_2 u_2(1-u_1-u_2) - \frac{a u_2 u_3}{1+b(u_1+u_2)} + \lambda \frac{u_1 u_2}{u_1+u_2} - m_2 u_2, \quad (22b)$$

$$f_3 = \frac{a(u_1+u_2)u_3}{1+b(u_1+u_2)} - m_3 u_3. \quad (22c)$$

Proportionate mixing with transmission coefficient λ as well as an additional disease-induced mortality of infected (virulence) with rate m_2 are assumed. The vector of population densities is $\mathbf{u}=(u_1,u_2,u_3)$. In the case of lytic infection, the first term on the right-hand side of Equation (22b) would describe the losses due to natural mortality and competition. Here, lysogenic infections with $\gamma_1=\gamma_2=\gamma$ will be considered.

For $m_2 > \lambda$, the infected go extinct, for $m_2 < \lambda$, the susceptibles do. In the case of $m_2=\lambda$, susceptibles and infected coexist (endemic states). Because of the symmetry of the growth terms of susceptibles and infected, the initial conditions determine their final dominance in the endemic state, i.e., if $u_1(t=0) > u_2(t=0)$ then $u_1(t) > u_2(t)\ \forall\ t$. The prevalence $i=u_2(t)/(u_1(t)+u_2(t))$ remains constant (Malchow et al. 2004).

Furthermore, multiplicative noise is introduced in Equations (22) in order to study environmental fluctuations, i.e.,

$$\frac{\partial u_i(\mathbf{r},t)}{\partial t} = f_i[\mathbf{u}(\mathbf{r},t)] + d\nabla^2 u_i(\mathbf{r},t) + \omega_i[\mathbf{u}(\mathbf{r},t)]\cdot\xi_i(\mathbf{r},t), i=1,2,3; \quad (23)$$

where $\xi_i(\mathbf{r},t)$ is a spatiotemporal white Gaussian noise, i.e., a random Gaussian field with zero mean and delta correlation

$$\langle\xi_i(\mathbf{r},t)\rangle = 0, \langle\xi_i(\mathbf{r}_1,t_1)\xi_i(\mathbf{r}_2,t_2)\rangle = \delta(\mathbf{r}_1-\mathbf{r}_2)\delta(t_1-t_2), i=1,2,3. \quad (23a)$$

$\omega_i[\mathbf{u}(\mathbf{r},t)]$ is the density dependent noise intensity. The stochastic modelling of population dynamics requires this density dependence, i.e., multiplicative noise. Throughout this paper, it is chosen as

$$\omega_i[\mathbf{u}(\mathbf{r},t)] = \omega u_i(\mathbf{r},t), i=1,2,3; \omega = \text{const.} \quad (23b)$$

We consider the spatiotemporal dynamics of the plankton model (23), i.e., zooplankton, grazing on susceptible and virally infected phytoplankton, under the influence of environmental noise and diffusing in horizontally two-dimensional space. The diffusion terms have been integrated using the semi-implicit Peaceman–Rachford alternating direction scheme, cf. Thomas (1995). For the interactions and the Stratonovich integral of the noise terms, the explicit Euler–Maruyama scheme has been applied (Kloeden and Platen 1992; Higham 2001). Periodic boundary conditions have been chosen for all simulations.

The initial conditions are localized patches in empty space, and they are the same for deterministic and stochastic simulations. Two initial configurations have been considered and they can be seen in Figures 13 and 15. In the first case, cf. Figure 13, there are two patches, one with zooplankton surrounded by susceptible phytoplankton (upper part of the model area) and one with zooplankton surrounded by infected ones (on the right of the model area). In the second case, cf. Figure 16, there is a central patch of all three species; inside this patch the susceptibles are ahead of infected which are ahead of zooplankton.

The simulation results are shown in Figures 14 and 16 which were obtained for the initial conditions shown in Figures 13 and 15, respectively. The first two rows show the dynamics of the

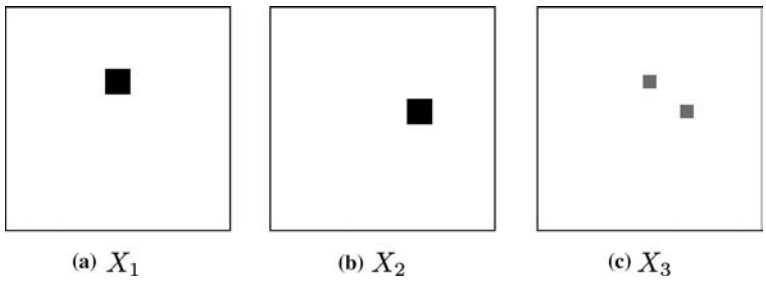

Figure 13. Initial conditions for the simulations in Figure 14. Upper left patch: Zooplankton surrounded by susceptibles. Lower right patch: Zooplankton surrounded by infected.

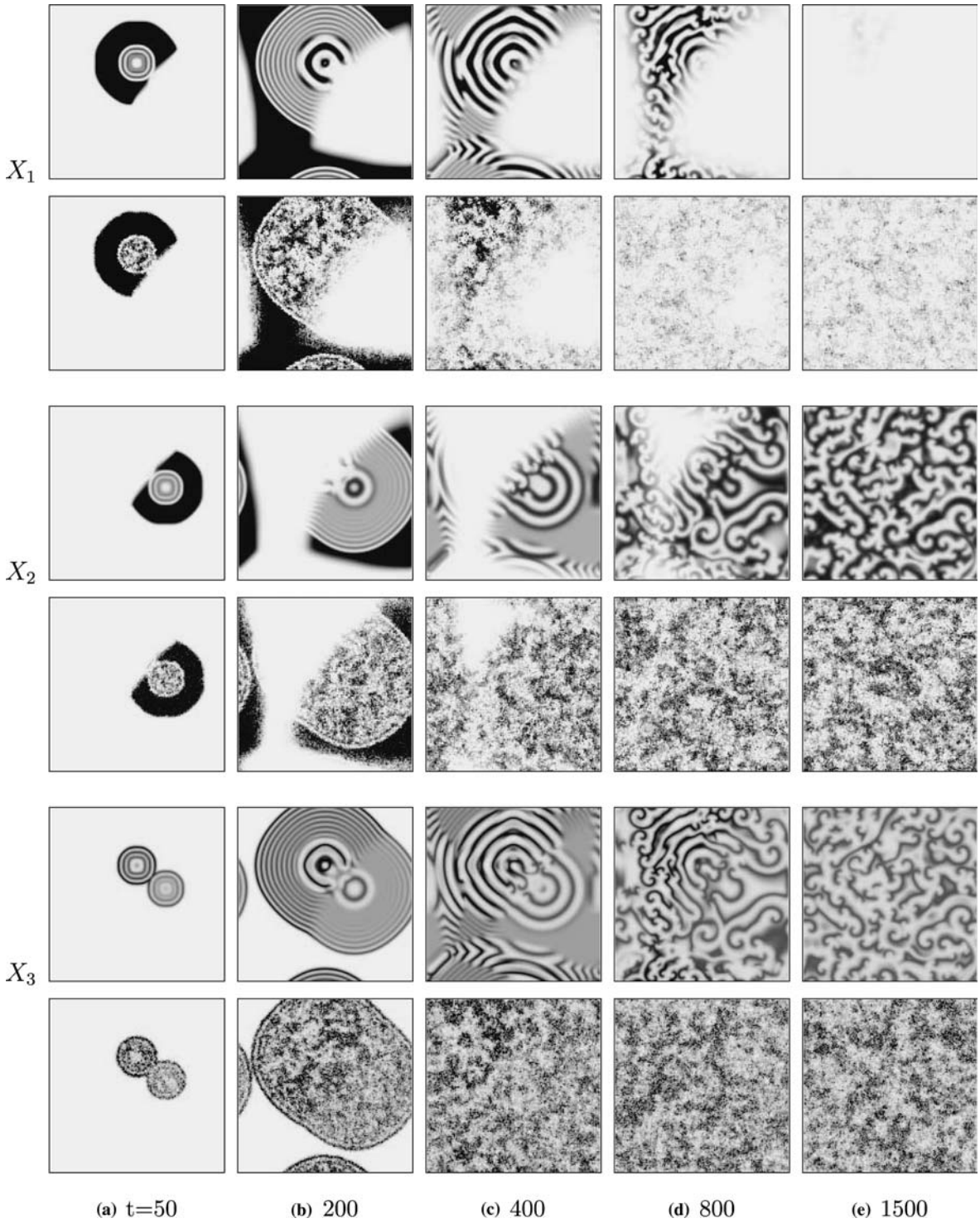

Figure 14. Invasion and spatial coexistence of infected (two middle rows) and zooplankton (two lower rows). Extinction of susceptibles (first row) without noise. Survival and patchy invasion of susceptibles for $\omega = 0.25$ noise intensity (second row). Parameters are: $m_2 = 0.2 < \Lambda = 0.21$, $m_3 = 0.5$, $d = 0.05$.

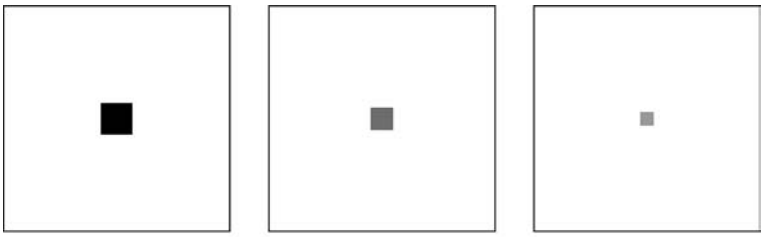

Figure 15. Initial conditions for the simulations in Figure 16. Zooplankton surrounded by infected surrounded by susceptibles.

susceptibles for deterministic and stochastic conditions, the two middle rows show the infected and the two lower rows the zooplankton. In both figures, this special initial configuration leads at first to the propagation of concentric waves for the deterministic case in rows 1, 3 and 5. For the stochastic case in rows 2, 4 and 6, these waves are immediately blurred and only a leading diffusive front remains. The grey scale of the figures changes from high population densities in dark colour to vanishing densities in white.

In Figure 14, it can be observed that the susceptibles go extinct in the deterministic case for $m_2 < \lambda$. Any supercritical environmental fluctuation could initiate the switch to the lytic viral replication cycle, and all populations would go extinct. However, the noise enhances the survival and patchy invasion of susceptibles even under unfavourable conditions, cf. the second row in Figure 14.

In Figure 16, one can see the final spatial coexistence of all three species for $m_2 = \lambda$. The deterministic simulations yield the dynamic stabilization of the locally unstable focus in space and a long plateau is formed with a leading diffusive front ahead, cf. (Petrovskii and Malchow 2000; Malchow and Petrovskii 2002). Furthermore, in the purely deterministic case the infected are somehow trapped in the center and go almost extinct. The noise enhances the 'escape', survival and patchy invasion of the infected, cf. the fourth row in Figure 16.

Conclusions

In this paper we have revisited the phenomenon of patchy invasion which was observed earlier in (Petrovskii et al. 2002a, b). The patterns of patchy spread in nature are usually attributed either to environmental heterogeneity (cf. Murray 1989) or to environmental stochasticity (Lewis 2000; Lewis and Pacala 2000). In contrast, we have shown that the patchy spread of an exotic species can take place in a homogeneous environment and regardless of the existence/importance of stochastic factors. In a purely deterministic system, the patchy invasion can arise as a 'response' of the invasive species to the measures of biological control based on intentional introduction of a specialist predator or infection disease, provided that the local population growth of the exotic species is damped by the strong Allee effect.

By means of extensive numerical simulations (only a small number of them are shown in Figures 1–4, 6–11), the following facts have been proved:

1. Patchy invasion must not be associated with a specific model but should be regarded as a more general phenomenon that can be observed in various systems of population dynamics and epidemiology;
2. Patchy invasion is a mechanism of species spread 'at the edge of extinction': a small change of controlling parameters can bring given invasive species to extinction;
3. For those parameter values when the patchy invasion takes place in the 2-D system, in the corresponding 1-D system the species go extinct.

The impact of stochastic factors can significantly modify the system's spatiotemporal dynamics, see e.g. (Malchow et al. 2002, 2004). In the model of virally infected plankton, the ratio of virulence and infection transmission rate controls coexistence, survival or extinction of

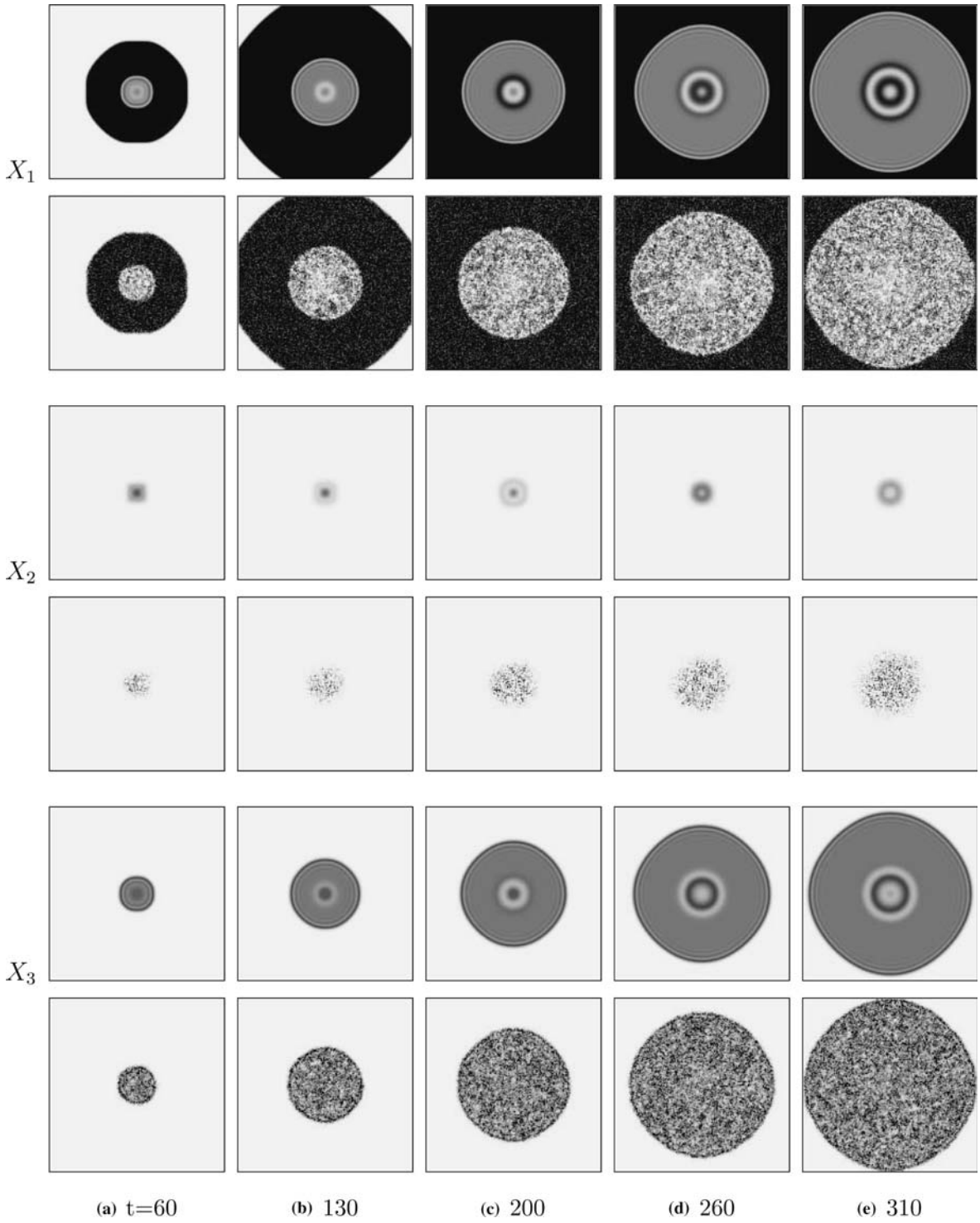

Figure 16. Spatial coexistence of susceptibles (two upper rows), infected (two middle rows) and zooplankton (two lower rows). Trapping and almost extinction of infected in the center (third row) without noise. With $\omega = 0.25$ noise intensity noise-enhanced survival and patchy invasion of infected (fourth row). Phenomenon of dynamic stabilization of a locally unstable equilibrium (first and fifth row).The definition of the subfigures in the third row is sharpened three times, in the fourth row two times. Parameters are: $m_2 = \Lambda = 0.2$, $m_3 = 0.625$, $d = 0.05$.

susceptibles and infected in a non-fluctuating environment. A sufficiently large environmental noise enhances the survival and the patchy spatial spread of the 'endangered' species. Stochasticity relaxes the conditions for patchy invasion so that it can also be observed in a system without Allee effect. If considered in a wider ecological perspective, the latter conclusion seems to be congenial to the results obtained by Lande (1998) who showed that the Allee effect can originate in the stochasticity inherent in populations at small density. In general, however, the interplay between deterministic and stochastic factor and its impact on the dynamics of invasive populations is not well understood yet. This problem will become a subject of future studies.

Acknowledgements

The authors wish to express their gratitude to Andrew Morozov (Moscow) and Michel Langlais (Bordeaux) for fruitful discussions of the problem, and to Franck Courchamp (Paris) and Fugo Takasu (Nara) for valuable comments made in order to improve the manuscript's clarity. This work was partially supported by Deutsche Forschungsgemeinschaft (DFG) under Grant 436 RUS 113/631 and by Russian Foundation for Basic Research under Grant 03-04-48018. S.P. is also thankful to EU TEMPUS program, Grant IMG-03-RF-2013.

References

Abramson G, Kenkre V, Yates T and Parmenter R (2003) Traveling waves of infection in the Hantavirus epidemics. Bulletin of Mathematical Biology 65: 519–534

Allen L (2003) An Introduction to Stochastic Processes with Applications to Biology. Pearson Education, Upper Saddle River, NJ, 424 pp

Anishenko V, Astakov V, Neiman A, Vadivasova T and Schimansky-Geier L (2003) Nonlinear Dynamics of Chaotic and Stochastic Systems. Tutorial and Modern Developments. Springer Series in Synergetics. Springer, Berlin, 530 pp

Beltrami E and Carroll TO (1994) Modeling the role of viral disease in recurrent phytoplankton blooms. Journal of Mathematical Biology 32: 857–863

Chattopadhyay J and Pal S (2002) Viral infection on phytoplankton–zooplankton system – a mathematical model. Ecological Modelling 151: 15–28

Chattopadhyay J, Sarkar R and Pal S (2003) Dynamics of nutrient–phytoplankton interaction in the presence of viral infection. BioSystems 68: 5–17

Courchamp F and Sugihara G (1999) Biological control of alien predator populations to protect native island prey species from extinction. Ecological Applications 9: 112–123

Diekmann O and Heesterbeek JAP (2000) Mathematical Epidemiology of Infectious Diseases: Model Building, Analysis and Interpretation.Wiley, Chichester, 388 pp

Dietz K and Schenzle D (1985) Proportionate mixing models for age-dependent infection transmission. Journal of Mathematical Biology 22: 117–120

Drake JA, Mooney HA, di Castri F, Groves RH, Kruger FJ, Rejmanek M and Williamson M (eds) (1989) Biological Invasions: Global Perspective. John Wiley, New York, 656 pp

Fagan WF and Bishop JG (2000) Trophic interactions during primary succession: herbivores slow a plant reinvasion at Mount St. Helens. American Naturalist 155: 238–251

Fitzgerald BM and Veitch CR (1985) The cats of Herecopare Island, New Zealand: their hystory, ecology and effects on birdlife. New Zealand Journal of Zoology 12: 319–330

Fuhrman J (1999) Marine viruses and their biogeochemical and ecological effects. Nature 399: 541–548

Gastrich MD, Leigh-Bell JA, Gobler CJ, Anderson OR, Wilhelm SW and Bryan M (2004) Viruses as potential regulators of regional brown tide blooms caused by the alga, *Aureococcus anophagefferens*. Estuaries 27: 112–119

Grenfell B, Bjørnstad O and Kappey J (2001) Travelling waves and spatial hierarchies in measles epidemics. Nature 414: 716–723

Hethcote HW (2000) The mathematics of infectious diseases. SIAM Review 42: 599–653

Higham D (2001) An algorithmic introduction to numerical simulation of stochastic differential equations. SIAM Review 43: 525–546

Holmes EE, Lewis MA, Banks JE and Veit RR (1994) Partial differential equations in ecology: spatial interactions and population dynamics. Ecology 75: 17–29

Jacquet S, Heldal M, Iglesias-Rodriguez D, Larsen A, Wilson W and Bratbak G (2002) Flow cytometric analysis of an *Emiliana huxleyi* bloom terminated by viral infection. Aquatic Microbial Ecology 27: 111–124

Jiang S and Paul J (1998) Significance of lysogeny in the marine environment: studies with isolates and a model of lysogenic phage production. Microbial Ecology 35: 235–243

Keitt TH, Lewis MA and Holt RD (2001) Allee effects, invasion pinning, and species borders. American Naturalist 157: 203–216

Kloeden P and Platen E (1992) Numerical Solution of Stochastic Differential Equations. Applications of Mathematics. Volume 23, Springer, Berlin, 512 pp

Lande R (1998) Demographic stochastisity and Allee effect on a scale with isotropic noise. Oikos 83: 353–358

Lewis MA (2000) Spread rate for a nonlinear stochastic invasion. Journal of Mathematical Biology 41: 430–454

Lewis MA and Kareiva P (1993) Allee dynamics and the spread of invading organisms. Theoretical Population Biology 42: 141–158

Lewis MA and Pacala S (2000) Modeling and analysis of stochastic invasion processes. Journal of Mathematical Biology 41: 387–429

Lin J, Andreasen V, Casagrandi R and Levin S (2003) Traveling waves in a model of influenza A drift. Journal of Theoretical Biology 222: 437–445

Malchow H and Petrovskii SV (2002) Dynamical stabilization of an unstable equilibrium in chemical and biological systems. Mathematical and Computer Modelling 36: 307–319

Malchow H, Petrovskii SV and Medvinsky AB (2002) Numerical study of plankton-fish dynamics in a spatially structured and noisy environment. Ecological Modelling 149: 247–255

Malchow H, Hilker F, Petrovskii SV and Brauer K (2004) Oscillations and waves in a virally infected plankton system, I. The lysogenic stage. Ecological Complexity 1: 211–223

McCallum H, Barlow N and Hone J (2001) How should pathogen transmission be modelled? Trends in Ecology and Evolution 16: 295–300

Medvinsky AB, Petrovskii SV, Tikhonova IA, Malchow H and Li BL (2002) Spatiotemporal complexity of plankton and fish dynamics. SIAM Review 44: 311–370

Morozov AY, Petrovskii SV and Li BL (2004) Bifurcations and chaos in a predator–prey system with the Allee effect. Proceedings of Royal Society of London B 271: 1407–1414

Murray JD (1989) Mathematical Biology. Springer, Berlin. 849 pp

Nisbet RM and Gurney WSC (1982) Modelling Fluctuating Populations. Wiley & Sons, Chichester, 398 pp

Nold A (1980) Heterogeneity in disease-transmission modeling. Mathematical Biosciences 52: 227–240

Ortmann A, Lawrence J and Suttle C (2002) Lysogeny and lytic viral production during a bloom of the cyanobacterium *Synechococcus* sp. Microbial Ecology 43: 225–231

Owen M and Lewis MA (2001) How predation can slow, stop or reverse a prey invasion. Bulletin of Mathematical Biology 63: 655–684

Parker IM, Simberloff D, Londsdale WM, Goodell K, Wonham M, Kareiva PM, Williamson MH, Von Holle B, Moyle PB, Byers JE and Goldwasser L (1999) Impact: toward a framework for understanding the ecological effects of invaders. Biological Invasions 1: 3–19

Pascual M (1993) Diffusion-induced chaos in a spatial predator–prey system. Proceedings of Royal Society of London B 251: 1–7

Petrovskii SV and Malchow H (2000) Critical phenomena in plankton communities: KISS model revisited. Nonlinear Analysis: Real World Applications 1: 37–51

Petrovskii SV and Venturino E (2004) Patterns of patchy spatial spread in models of epidemiology and population dynamics. University of Torino, preprint #20/2004 (available online: http://www.dm.unito.it/quadernidipartimento/quaderni.php)

Petrovskii SV, Morozov AY and Venturino E (2002a) Allee effect makes possible patchy invasion in a predator–prey system. Ecology Letters 5: 345–352

Petrovskii SV, Vinogradov ME and Morozov AY (2002b) Spatio-temporal horizontal plankton patterns caused by biological invasion in a two-species model of plankton dynamics allowing for the Allee effect. Oceanology 42: 384–393

Petrovskii SV, Malchow H and Li BL (2005a) An exact solution of a diffusive predator–prey system. Proceedings of Royal Society of London A 461: 1029–1053

Petrovskii SV, Morozov AY and Li BL (2005b) Regimes of biological invasion in a predator–prey system with the Allee effect. Bulletin of Mathematical Biology 67: 637–661

Pimentel D (2002) Biological Invasions: Economic and Environmental Costs of Alien Plant, Animal and Microbe Species. CRC Press, New York, 524 pp

Scheffer M (1991) Fish and nutrients interplay determines algal biomass: a minimal model. Oikos 62: 271–282

Sherratt JA (2001) Periodic travelling waves in cyclic predator–prey systems. Ecology Letters 4: 30–37

Sherratt JA, Lewis MA and Fowler AC (1995) Ecological chaos in the wake of invasion. Proceedings of US National Academy of Science 92: 2524–2528

Shigesada N and Kawasaki K (1997) Biological Invasions: Theory and Practice. Oxford University Press, Oxford, 205 pp

Suttle C (2000) Ecological, evolutionary, and geochemical consequences of viral infection of cyanobacteria and eukaryotic algae. In: Hurst C (ed) Viral Ecology, pp 247–296. Academic Press, San Diego

Tarutani K, Nagasaki K and Yamaguchi M (2000) Viral impachts on total abundance and clonal composition of the harmful bloom-forming phytoplankton *Heterosigma akashiwo*. Applied and Environmental Microbiology 66(11): 4916–4920

Thomas J (1995) Numerical partial differential equations: Finite difference methods. Texts in Applied Mathematics. Volume 22. Springer, New York, 477 pp

Volpert AI, Volpert VA and Volpert VA (1994) Travelling Wave Solutions of Parabolic Systems. American Mathematical Society, Providence, 455 pp

Vinogradov ME, Shushkina EA, Musaeva EI and Sorokin PY (1989) A new invader to the Black Sea – ctenophore *Mnemiopsis leidyi* (A. Agassiz) (Ctenophora Lobata). Oceanology 29: 293–299

Vinogradov ME, Shushkina EA, Anochina LL, Vostokov SV, Kucheruk NV and Lukashova TA (2000) Mass development of ctenophore Beroe ovata Eschscholtz off the north-eastern coast of the Black Sea. Oceanology 40: 52–55

Wommack K and Colwell R (2000) Virioplankton: viruses in aquatic ecosystems. Microbial Molecular Biology Review 64(1): 69–114

Zhdanov V (2003) Propagation of infection and the prey–predator interplay. Journal of Theoretical Biology 225: 489–492